Nucleic Acids Research

Nucleosome conformation: pH and organic solvent effects

M.Zama,* D.E.Olins, B.Prescott[a] and G.J.Thomas, Jr.[a]

University of Tennessee - Oak Ridge Graduate School of Biomedical Sciences and the Biology Division, Oak Ridge National Laboratory, Oak Ridge, TN 37830, and [a]Department of Chemistry, Southeastern Massachusetts University, North Dartmouth, MA 02747, USA

ABSTRACT

Monomer nucleosomes (v_1) from chicken erythrocyte nuclei were examined in aqueous buffers (8 > pH > 3) and in solvent mixtures (i.e., water and ethanol, ethylene glycol, dioxane, dimethyl sulfoxide, 2-methyl-2,4-pentanediol, polyethylene glycol, sucrose, or urea). Circular dichroism, laser Raman spectroscopy of v_1, and the fluoresence of v_1 labeled with N-(3-pyrene)maleimide on thiol groups of H3 histone were employed to detect conformational transitions in v_1. The results of the pH studies were as follows: 5.5 > pH > 4.8, suppression of DNA ellipticity and no change of histone α-helix; 4.6 > pH > 4.2 an irreversible increase in the B character of DNA, a slight loss of histone α-helix, and a parallel loss of pyrene excimer fluorescence; 4 > pH, aggregation of v_1 and protonation of the DNA bases C and A. Results obtained in the studies of v_1 in solvent mixtures included the following: sharp conformational transitions that variously involved an increase in the B character of DNA, a slight loss of histone α-helix, and a loss of pyrene excimer. Different solvents required different concentrations to effect these conformational changes.

INTRODUCTION

Our present understanding of nucleosome structure is based primarily upon studies conducted in vitro. Recent biochemical studies suggest, however, that nucleosome conformation is altered in chromatin that is active in transcription (1–3). As an approach to identifying the conformational states or transitions of nucleosomes, extensive studies of the effects of urea and ionic strength on nucleosome structure were made previously (4–6).

In this paper we report the effects of pH and various organic solvents on nucleosome conformations. Circular dichroism and laser Raman spectroscopy were applied to identify changes of secondary structure in histones and DNA. The fluorescence of N-(3-pyrene)maleimide (NPM), which was covalently labeled to a cysteine residue at position 110 in chicken erythrocyte H3, has also been used effectively as a sensitive probe of nuclesome conformation.

METHODS

Preparation of Nucleosomes

Monomer nucleosomes (ν_1) from chicken erythrocytes were obtained by use of methods previously described (7,8). For most studies the KCl-soluble nucleosomes were employed. These were stored frozen at -20° in 0.2 m$\underline{M}$ EDTA, pH 7.0 ($A_{260} \sim 130$), then diluted with the appropriate buffer solutions or solvent mixtures just before use.

Preparation of Nucleosomes Labeled with NPM

Mononucleosomes (0.16 mg/ml or 7.4×10^{-7} $\underline{M}$ assuming a molar extinction coefficient $\epsilon_{\nu_1, 260} = 1.9 \times 10^6$) in 1.4 $\underline{M}$ KCl, 0.2 m$\underline{M}$ EDTA (pH 7.0) were mixed with NPM (Polyscience, Inc.) at 10^{-5} $\underline{M}$, which was diluted from a stock solution of 10^{-2} $\underline{M}$ in dimethyl sulfoxide, and incubated for 60 min at 37°. Following the reaction, the entire mixture was dialyzed for 5 hr at 4° against 1.4 $\underline{M}$ KCl, 0.2 m$\underline{M}$ EDTA. The labeled complex (NPM–ν_1) was reassociated by step-gradient dialysis for 4–6 hr against, 1.0, 0.4, 0.3, and 0.1 $\underline{M}$ KCl in sequence, each containing 0.2 m$\underline{M}$ EDTA. This was followed by dialysis against 0.2 m$\underline{M}$ EDTA for 16–18 hr. The dialyzed NPM–ν_1 solution was centrifuged (10 min, 27,000 x g) to remove any aggregates; then the NPM–ν_1 complexes were subfractionated by sucrose-gradient ultracentrifugation to obtain "good" particles (5). These "good" particles were dialyzed against 0.2 m$\underline{M}$ EDTA (pH 7.0) and stored frozen in small aliquots at -20°. The fluorescence and other properties of NPM–ν_1 complexes have been described elsewhere (5).

Spectrophotometric Measurements

Absorption was measured on a Zeiss PMQ II spectrophotometer. Circular dichroism measurements were performed on a Jasco J-40A spectropolarimeter at room temperature. The molar extinction coefficient at 260 nm of DNA ($\epsilon_p = 6500$) was used in calculations of the molar ellipticity expressed as moles of nucleotides, $[\theta]_p$.

Fluorescence emission spectra of NPM–ν_1 complex in solutions of different pH or in different solvents were measured with Aminco-Bowman and Perkin-Elmer MPF–44 recording spectrofluorometers. Solutions of NPM–ν_1 complexes always had an absorption of less than 0.01 at the excitation wavelength, 340 nm. The fluorescence contribution from any organic solvent was subtracted from the fluorescence of the NPM–ν_1 complex in the corresponding solvent.

Laser Raman Spectra of ν_1 and solvents were obtained with 488.0-nm excitation from an argon ion laser (Coherent Model CR2) and were recorded on a Spex Ramalog

spectrophotometer. Details of Raman instrumentation and sample handling for Raman spectroscopy have already been described (9,10).

Solvents

Standard buffers (Tris-HCl, cacodylate, acetate, and glycine-HCl) were employed to cover the range 9>pH>2. Buffer concentrations of 4.75 and 0.5 m$\underline{M}$ were used for DNA and for v_1, respectively.

Ethanol, ethylene glycol, dimethyl sulfoxide, 2-methyl-2,4-pentanediol, and polyethylene glycol were reagent grade. 2-methyl-2,4-pentanediol was distilled prior to use. Polyethylene glycol (MW 4000 and 6000) was purified by ether precipitation from ethanol to remove impurities absorbing in the UV. Dioxane was of spectroquality. Sucrose was of ultrapure, density-gradient grade. Urea was of ultrapure grade. All aqueous/organic solvent mixtures contained 0.2 m$\underline{M}$ EDTA (pH 7.0).

RESULTS
Effects of pH

The absorbance and circular dichroism of DNA and v_1 were measured over the range 9>pH>2 (Fig. 1). As is well known (11), with decreasing pH, the absorbance of DNA at 260 nm is unchanged to pH 4.5, followed by a slight decrease between pH 4.5 and 3.5, and then an abrupt increase below pH 3.2. Correspondingly, DNA ellipticity ($[\theta]_{P,\,281}$) begins to decrease from pH 5 to 3.2, where a sharp increase is observed. The decrease in absorbance is attributed to protonation of bases without breakdown of the DNA secondary structure, and the increase is attributed to DNA strand separation. The initial decrease in $[\theta]_{P,281}$ indicates a change of the native DNA helical conformation, existing at pH 7, as a consequence of protonation of the DNA bases (12).

Mononucleosomes exhibit characteristic absorption and circular dichroism behavior as a function of pH. Several regions can be discerned: 7.5>pH>5.5, negligible changes in either DNA conformation ($[\theta]_{P,281}$) or the α-helix content of histones ($[\theta]_{P,223}$); 5.5>pH>4.8, "suppression" of DNA ellipticity but no apparent loss of histone α-helix; 4.6>pH>4.2, a sharp increase in DNA ellipticity towards the conformation of naked DNA in solution, with a slight loss of histone α-helix content (note that these circular dichroism changes are irreversible): 4.2>pH>3.8, aggregation of v_1, as evidenced by the increase in absorbance at 325 nm due to light
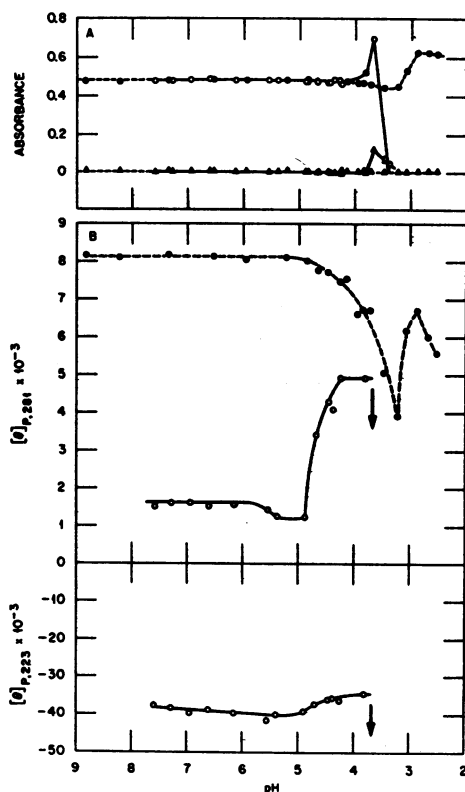
Figure 1. Absorption and circular dichroism of DNA and ν_1 as a function of pH.
(A) A_{260} for DNA ($\bullet$) and ν_1 ($\bigcirc$), A_{325} for DNA ($\blacktriangle$) and ν_1 ($\triangle$).
(B) $[\theta]_{P,281}$ for DNA ($\bullet$) and ν_1 ($\bigcirc$), $[\theta]_{P,223}$ for ν_1 ($\bigcirc$). 4.75 and 0.5 m$\underline{M}$
buffers were used for DNA and ν_1, respectively. Buffer solutions in the range
9>pH>2 were prepared by use of the following systems: Tris-HCl; sodium cacodylic
acid; sodium acetate–acetic acid, and glycine-HCl.

scattering, followed ultimately by precipitation of the aggregates from solution.
Representative circular dichroism spectra of DNA and ν_1 at different pH's are shown in
Fig. 2. The "suppressed" circular dichroism spectrum of ν_1 at pH 5.4, relative to the
spectrum at pH 7.6, can be seen. It is also apparent that the ellipticity of DNA within
ν_1 at pH 4.2 (Fig. 2A) is still suppressed compared with that of free DNA at pH 4.3
(Fig. 2B).

The fluorescence of NPM-labeled ν_1 is shown as a function of pH in Fig. 3.
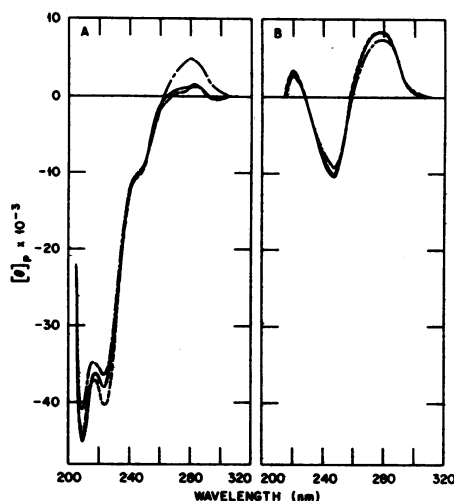Spectra of NPM-ν_1 complexes at pH 7.3 and pH 5.5 exhibit a long-wavelength excimer

Figure 2. Circular dichroism spectra of DNA and ν_1 at different pH's. (A) ν_1 at pH 7.6 (—), 5.4 (----), and 4.2 (— - —). (B) DNA at pH 7.3 (—), 5.2 (---), and 4.3 (— - —).

fluorescence at 450 nm as well as monomer fluorescence at 375 and 395 nm, as reported previously (5). On the other hand, at pH 4.3 the excimer band disappears and intensified monomer bands are observed (Fig. 3B). Plots of relative fluorescence intensity versus pH (Fig. 3A) show slight intensity changes down to pH 4.5, where a simultaneous sharp decrease of excimer and increase of monomer fluorescence occur. In this pH region (i.e., the 4.6>pH>4.2 region in Fig. 1B) parallel changes in circular dichroism occur for both DNA and histones. The excimer fluorescence of NPM–ν_1 complex, believed to arise from pairwise association of pyrene groups attached to the thiols of H3 histone within ν_1, has proven to be a remarkably sensitive probe of nucleosome conformational changes (5). Presumably this sensitivity arises from the stringent geometric constraints required for energy transfer within the excited state. Thus the fluorescence changes at pH ~4.5 suggest the existence of conformational changes of ν_1 which lead to disruption of stacking between NPM molecules within ν_1.

Laser Raman spectra of chicken DNA and ν_1 are shown in Figs. 4A and 4B, respectively, for the range 7>pH>2. Similar spectra for DNA and ν_1 at neutral pH have been reported and discussed previously (9).

In the range 7>pH>5 no large changes occur in Raman line frequencies or

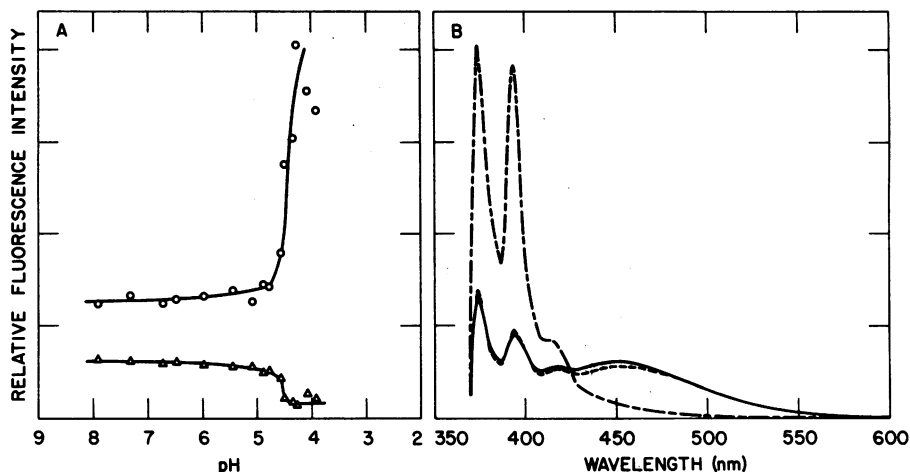Figure 3. Fluorescence of NPM-labeled ν_1 as a function of pH. (A) Fluorescence intensities at 450 ($\triangle$) and 375 nm ($\bigcirc$). (B) Fluorescence spectra at pH 7.3 (——), 5.5 (----), and 4.3 (— - —). 0.45 mM buffers were used.

intensities of either DNA or ν_1. Therefore no substantial changes in structures of free DNA or ν_1 are occurring in this pH range from the standpoint of Raman spectroscopy. Near pH 4, however, the Raman lines of neutral cytosine (C) and adenine (A) rings (13) lose intensity relative to their peak heights at pH>5, and simultaneously new Raman lines associated with protonated cytosine (C^+) and protonated adenine (A^+) (13, 14) appear in the spectra of Fig. 4. Thus substantial protonation of the bases A and C occurs in DNA at pH 3.9 (Fig. 4A) and in ν_1 at pH 3.8 (Fig. 4B). Protonation of these bases is extensive by pH 2.8. We can detect only a small modulating effect of the bound histones upon the degree of base protonations in DNA of ν_1 as a function of pH.

The Raman spectrum of DNA also exhibits several lines which are sensitive to the conformation of the DNA backbone. Among these are the line at 832 cm^{-1} which is assigned to a vibration of the phosphodiester group, and the line near 675 cm^{-1} which is actually composed of an overlapping pair (doublet) of lines at 671 and 681 cm^{-1}, due, respectively, to ring vibrations of thymine and guanine residues (10, 15–18). At higher spectral resolution than employed for the present study, the doublet is more clearly resolved into its two components (see, for example, refs. 10 and 18).

For the present case (Fig. 4A) we see that the line at 832 cm^{-1} gradually
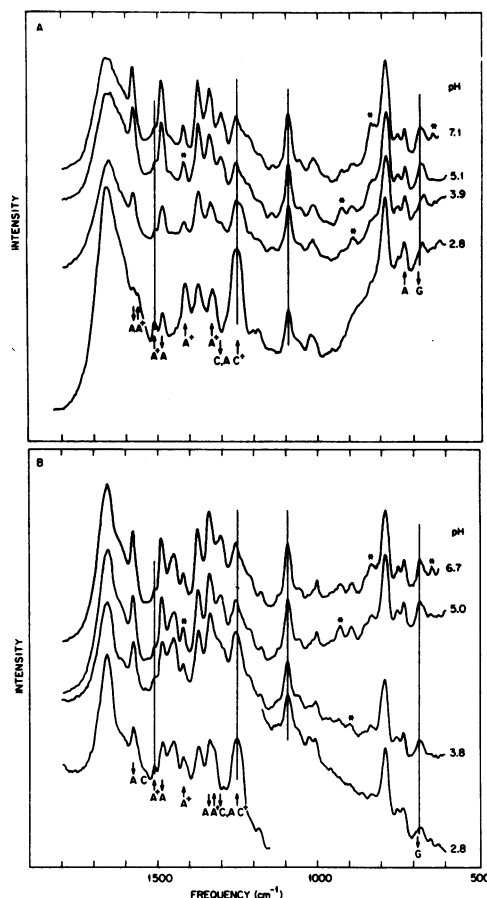
Figure 4. (A) Raman spectra of chicken DNA (4% by weight) at different pH's. All spectra were obtained at 32°. An asterisk indicates a Raman band due in whole or in part to buffer. An arrow indicates the direction of change of Raman band intensity, with decreasing pH. Letter symbols indicate DNA base residues. Vertical lines show the protonation of A and C (1510 and 1250 cm^{-1}, respectively), the denaturing of DNA via G (681 cm^{-1}), and the absence of a change in the 1094 cm^{-1} phosphate line. The following buffers were used: 0.02 M cacodylate (pH 7.1); 0.02 M acetate (pH 5.1); 0.02 M acetate (pH 3.9); 0.02 M glycine–HCl (pH 2.8). (B) Raman spectra of nucleosomes (10–13% by weight) at different pH's. The following buffers were used: 0.02 M cacodylate (pH 6.7); 0.02 M acetate (pH 5.0); 0.02 M acetate (pH 3.8); 0.02 M glycine-HCl (pH 2.8). At 4 > pH the spectrum is of a precipitate. All spectra were obtained at 32°. The notations of the symbols are the same as in Fig. 4A.

diminishes in intensity as the pH is lowered to 3.9. The line at 832 cm^{-1} is barely detectable at pH 2.8, suggesting a major change of secondary structure at this pH. Similarly, the 671/681 cm^{-1} doublet appears to be shifted to lower frequency with decreasing pH, an observation which is explained by the fact that the thymine component (671 cm^{-1}) greatly increases in intensity relative to the guanine component (681 cm^{-1}) at low pH. Identical effects have been observed to accompany the thermal denaturation of DNA and have been explained in terms of a loss of the B-genus DNA secondary structure. The present findings are therefore best explained in the following manner: As the solution pH is lowered, the bases A and C become protonated and the B-genus DNA secondary structure is gradually eliminated. Comparison of Fig. 4B with Fig. 4A shows that the histones bound to DNA in v_1 do not greatly attenuate the degree of base protonation but do restrict the collapse of B-genus DNA structure as the pH is lowered. Thus the 832 cm^{-1} line and the 671/681 cm^{-1} doublet are not as greatly altered in v_1 (Fig. 4B) as in free DNA (Fig. 4A) for 7>pH>4.

Effects of Organic Solvents

The effects of ethanol, ethylene glycol, dimethyl sulfoxide, and dioxane on the circular dichroism of DNA and v_1 are shown in Fig. 5. Figure 6 presents the circular dichroism spectra of DNA and v_1 at different ethanol concentrations. Figure 7 illustrates effects of the various organic solvents on the fluorescence of NPM-v_1 complexes. From the standpoint of circular dichroism and fluorescence spectrocopy, the data of Figs. 5 and 7 show that organic solvents induce sharp conformational transitions in v_1. Specifically, these are an increase in the B character of DNA, accompanied by: concomitant slight loss (in ethanol and dioxane) or slight gain (in ethylene glycol) of histone α-helix content; and loss of excimer fluorescence, with increase of monomer fluorescence. Other solvent systems (sucrose, polyethylene glycol, and 2-methyl-2,4-pentanediol) were also used for the fluorescence studies of NPM-v_1 complexes (data not shown).

The Raman spectra of several solvent systems (dimethyl sulfoxide, urea, ethanol, and ethylene glycol) are presented in Fig. 8, in which "window" regions are indicated by the open boxes. These window regions illustrate how the Raman effect may be profitably employed to study conformational changes in v_1 when the corresponding solvent system is employed. Figure 9 presents the laser Raman spectra of DNA and v_1 in ethanol, dimethyl sulfoxide and urea solutions. All of our current data on the effects of specific solvent systems upon v_1 conformation are summarized as follows:
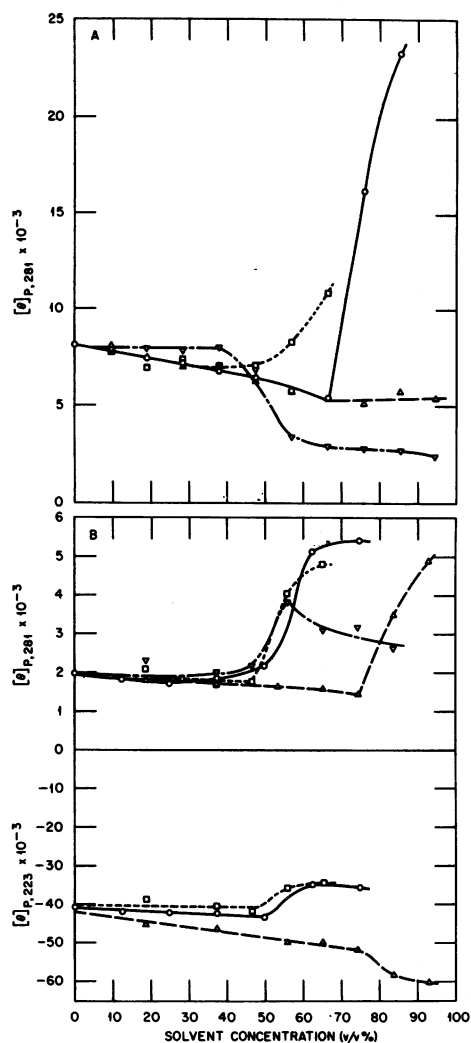
Figure 5. Circular dichriosm of DNA and ν_1 as a function of concentration of organic solvents (v/v%). (A) $[\theta]_{P,281}$ of DNA, (B) $[\theta]_{P,281}$ and $[\theta]_{P,223}$ of ν_1. Solvents: ethanol (◯), ethylene glycol (△), dioxane (□), and dimethyl sulfoxide (▽). All solvents contained 0.2 mM EDTA (pH 7.0).

Ethanol. Up to 50% ethanol there are no appreciable circular dichroism changes for either DNA or histone α-helix. An increase in the B character of DNA and a slight loss of α-helix in ν_1 occurs at 50–60% ethanol (Fig. 5B). These structural changes are irreversible. On the other hand, the excimer fluorescence disappears at
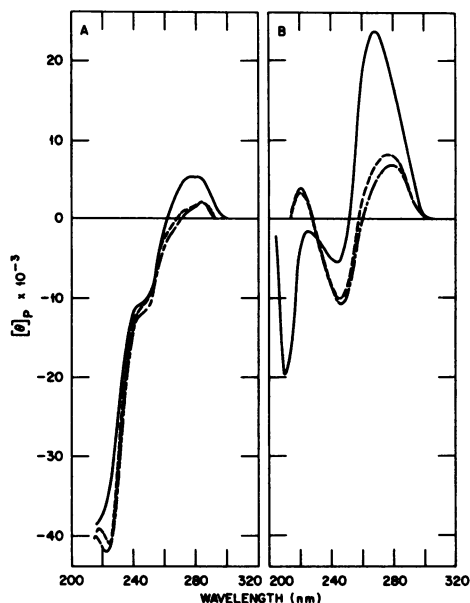
Figure 6. Circular dichroism spectra of DNA and v_1, at different ethanol concentrations. (A) v_1 in 0 (----), 37 (— - —), and 75% (——) ethanol. (B) DNA in 0 (----), 38 (———), and 76% (——) ethanol.

30—50% ethanol (Fig. 7A, B). The latter fact suggests that some tertiary or quaternary structural changes in the histones occur prior to the conformational change detected by circular dichroism. It is of interest that the magnitude of $[\theta]_{P,281}$ of v_1 in ethanol never increases to that of free DNA in the absence of ethanol. In contrast, free DNA exhibits a sharp transition from "B to A-like" conformation above 70% ethanol (Fig. 5A and 6B), as has been reported by other workers (19, 20).

The laser Raman spectrum of DNA in 80% ethanol (Fig. 9A) shows a prominent band at 807 cm^{-1} which is ascribed to the presence of "A-form DNA" (21), thus confirming the "B→A" transition. The Raman spectrum of v_1 in 80% ethanol differs among different samples, i.e., some samples show a very weak band at 807—811 cm^{-1} (Fig. 9A) but others did not. These results seem to indicate that DNA in v_1 possesses a conformational constraint which inhibits the transition to "A character" in ethanol. Finally in 50—60% ethanol solution the amide I Raman line of v_1 histones shifts to higher frequency (not shown in Fig. 9), confirming the loss of α-helical structure in the protein chains.
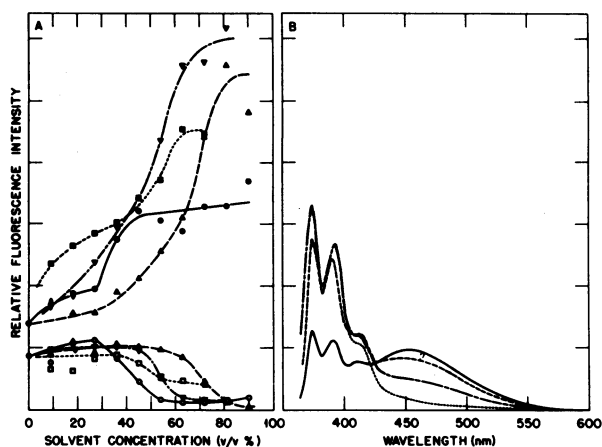
Figure 7. Fluorescence of NPM-labeled v_1 as a function of concentration of organic solvents (v/v%). (A) Fluorescence intensities at 460 nm (open symbols) and 374 nm (closed symbols), in ethanol ($\bigcirc$, $\bullet$), ethylene glycol ($\triangle$, $\blacktriangle$), dioxane ($\square$, $\blacksquare$) and dimethyl sulfoxide ($\triangledown$, $\blacktriangledown$). (B) Fluorescence spectra in 0 (—), 36 (– –), 45 (– - –), and 72% (----) ethanol.

Ethylene glycol. Mononucleosomes exhibit a slight decrease in $[\theta]_{P,281}$, as does free DNA (Fig. 5A), and in increase in $-[\theta]_{P,223}$ up to 75% ethylene glycol. These changes are followed by a sharp increase in $[\theta]_{P,281}$ and a simultaneous increase in $-[\theta]_{P,223}$ above 75% ethylene glycol (Fig. 5B). The absorbance (A_{260}) of free DNA increases above 65% ethylene glycol, indicative of denaturation, whereas no such indication of denaturation of the DNA in v_1 is observed. It is currently believed (22) that ethylene glycol preferentially disrupts hydrophobic interactions and adds stability to hydrogen bonds. In fact, an increase in the α-helical content of proteins in ethylene glycol has been observed for ß-lactoglobulin (23) and for the 50S subunit of ribosomes (24). The decrease of excimer fluorescence to a negligible intensity at 75% ethylene glycol precedes the sharp ciruclar dichroism changes, similar to the case of ethanol. Here, too, the circular dichroism changes above 75% ethylene glycol are found to be irreversible.

No changes are observed in the Raman spectra of v_1 or free DNA up to 80% ethylene glycol concentration.

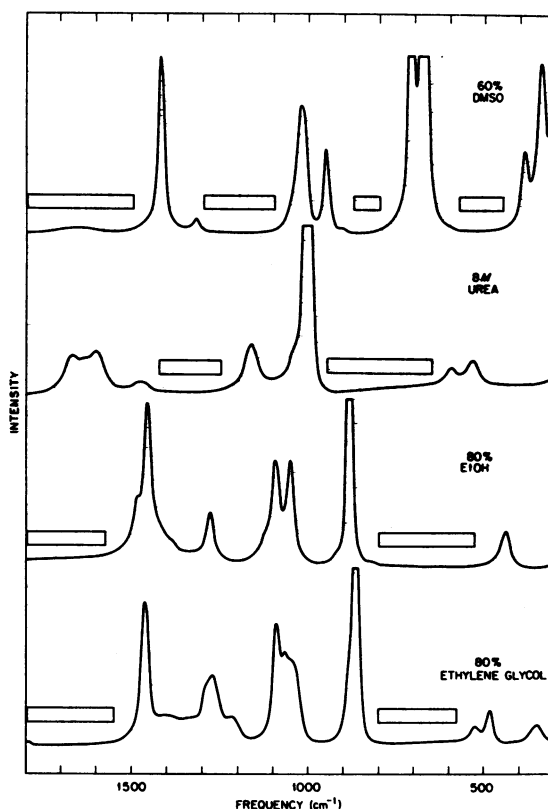Dimethyl sulfoxide. Dimethylsulfoxide (at 40% v/v) leads to denaturation of

Figure 8. Raman spectra of various solvent systems at 32°. Window regions are indicated by open boxes. From top to bottom, the solvents shown are: 60% dimethyl sulfoxide; 8 $\underline{M}$ urea; 80% ethanol; 80% ethylene glycol.

free DNA as shown by the decrease in $[\theta]_{P, 281}$ (Fig. 5A) and by an increase of A_{260} (data not shown). $[\theta]_{P, 281}$ of ν_1 begins to increase sharply at 45% dimethyl sulfoxide and then subsequently decreases sharply at 55%, most likely due to denaturation of DNA (Fig. 5B). The strong absorbance of dimethyl sulfoxide below 250 nm made it impossible to measure circular dichroism of ν_1 below ~250 nm.

In accord with these data, the Raman spectrum of DNA in 60% dimethyl sulfoxide exhibits spectral changes characteristic of denaturation (Fig. 9B). The amide I band of ν_1 shifts from 1658 to 1667 cm^{-1} in 45 and 60% dimethyl sulfoxide, respectively, consistent with either an α-helix → random coil or an α-helix → ß structure (or both) conformational changes (25). The shift of the strong band at 1257 to 1238 cm^{-1}
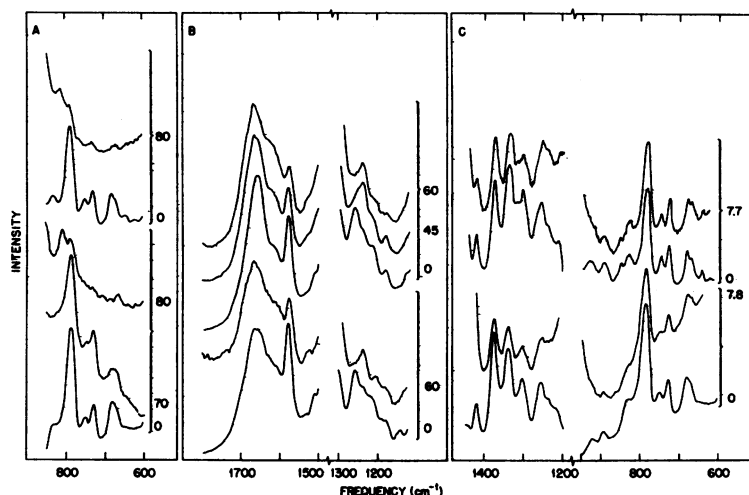
Figure 9. Raman spectra of DNA and ν_1 in various solvents containing 0.2 mM EDTA, at 32°. (A) top: ν_1 in 0 and 80% ethanol; bottom: DNA in 0, 70, and 80% ethanol. (B) top: ν_1 in 0, 45, and 60% dimethyl sulfoxide; bottom: DNA in 0 and 60% dimethyl sulfoxide. (C) top: ν_1 in 0 and 7.7 M urea; bottom: DNA in 0 and 7.8 M urea.

could arise from conformational changes in either DNA (base vibrations) or histones (amide III). The shift of amide I to higher frequency and the probable shift of amide III to lower frequency are greater in 60% than in 45% dimethyl sulfoxide. The absence of a strong amide III band ($\sim$1230 cm^{-1}, assignable to the ß conformation) in ν_1 in 45% dimethyl sulfoxide supports the view that in 45–60% dimethyl sulfoxide the DNA in ν_1 denatures with accompanying loss of α-helix in associated histones, and without any appreciable gain of ß structure.

A diminution of excimer fluorescence of NPM–ν_1 complexes is observed between 45 and 60 % dimethyl sulfoxide (Fig. 7A) and parallels the increase in the $[\theta]_{P,281}$ of ν_1.

Dioxane. We observe a sharp increase in the $[\theta]_{P,281}$ of ν_1 and a slight loss of α-helix between 45 and 60% dioxane (Fig. 5B). A parallel loss of excimer fluorescence is also noted in the same range of dioxane concentration (Fig. 7).

Urea. Raman bands of ν_1 in the amide I region are obscured by urea itself. Up to 5 M urea, however, no changes are observed in either the $\sim$600-900 or $\sim$1200–1400 cm^{-1}

cm^{-1} regions of the Raman spectrum, which are accessible (Fig. 9C). The spectral changes in the interval 1300–1400 cm^{-1} observed for ν_1 in 7.7 $\underline{M}$ urea are not observed for DNA in 7.8 $\underline{M}$ urea, suggesting that such changes are due to the histones. The Raman bands of ν_1 and DNA in the interval 650–850 cm^{-1} are unaffected by 7.7 $\underline{M}$ urea, which indicates no change in the B-genus DNA structure of ν_1. Previous studies of the effects of urea on ν_1 conformation have demonstrated the cooperative destruction of α-helix and unfolding of ν_1 particles at high urea concentrations (4). The present Raman data confirm the earlier findings.

Sucrose. Addition of up to ~40% sucrose causes no significant changes in the NPM–ν_1 complex fluorescence. This indicates that sucrose is not a perturbant to ν_1 conformation, from the standpoint of fluorescence spectroscopy.

Polyethylene glycol. The intensity of the excimer fluorescence of the NPM–ν_1 complex has a maximum value in 5–15% polyethylene glycol, with no significant loss of excimer intensity up to 45% polyethylene glycol. Thus, ν_1 probably maintains its compact structure in high concentrations of polyethylene glycol.

2-methyl-2,4-pentanediol. At 30-50% 2-methyl-2,4-pentanediol we observe a sharp loss of the excimer band and a simultaneous increase of the pyrene monomer bands of NPM–ν_1 complexes.

DISCUSSION

The present studies have shown that decreased pH and a variety of water-miscible organic solvents have perturbing effects on ν_1 conformation. A marked increase in the DNA ellipticity of ν_1, towards the conformation of naked DNA in solution, occurred at $4.6 > pH > 4.2$. Similar changes in DNA ellipticity were observed with ν_1 in various organic solvents. These DNA conformational changes have one feature in common, no matter what the perturbant is: they are accompanied by either a simultaneous slight decrease (lowered pH, ethanol, dioxane, and dimethyl sulfoxide) or a slight increase (ethylene glycol) of histone α-helix. In the cases examined (lowered pH, ethanol, and ethylene glycol) the changes induced in each solvent are irreversible. The slight change in α-helix content compared with the large changes in DNA conformation indicates that the α-helical regions are relatively more resistant than the DNA backbone to the perturbing effects of different solvent systems. Furthermore, the data on irreversibility suggest that the integrity of histone secondary structure may be an important part of the restoring force of nucleosomes, allowing the conformationally

perturbed nucleosome to return to its unperturbed conformation. The present results are consistent with those of our previous work (4) which showed that the different domains of nucleosome (i.e., the DNA-rich outer shell and the α-helix-rich apolar histone core) exhibit differential responsiveness to the chemical perturbant urea. In this respect, we have recently shown (26) that the two domains of nucleosome also respond differently to trypsin digestion (i.e., during the course of digestion with trypsin, a large increase in DNA ellipticity but virtually no decrease in the α-helix content of histones were observed).

In ethanol and in ethylene glycol solutions the loss of excimer fluorescence of NPM-labeled ν_1 preceded the circular dichroism changes of ν_1 and occurred at solvent concentration ranges at which no loss of α-helix content was observed. As in our previous study on the effects of urea on ν_1 (4, 5), these data suggest that the excimer fluorescence is a very sensitive indicator of ternary or quaternary structural changes of nucleosomes. We use the existence of the NPM excimer fluorescence as a measure of integrity of ν_1 conformation. For example, ν_1 conformation is highly susceptible to exposure to urea, losing the NPM excimer fluorescence in 0–3 $\underline{M}$ urea (5). Furthermore, judging by the maintenance of the NPM excimer fluorescence, ν_1 preserves its conformation intact up to 30% ethanol or 2–methyl–2,4–pentanediol, which were the strongest conformation perturbants among all the organic solvents examined in the present study. Within the solvent concentration ranges examined, sucrose ($\leq$ 40%) and polyethylene glycol ($\leq$ 45%) did not significantly affect the excimer fluorescence, apparently keeping ν_1 in its unperturbed conformation.

The nucleosome conformation was found to be stable over a pH range of 8> pH> 5. At about pH 5, a suppression of DNA ellipticity of ν_1, with no loss of α-helix, was observed. In this respect we note that Gordon et al. (27) have recently compared these circular dichroism observations with hydrodynamic properties of ν_1, and have concluded that the suppression of DNA ellipticity parallels a pH-induced increase in $S_{20,w}$ at low ionic strengths.

Laser Raman spectra have demonstrated that protonation of the bases C and A is not significant until below approximately pH 5. in DNA or pH 4 in ν_1. The mechanism which leads to the conformational changes of ν_1 at pH ~5 is not understood. Weintraub et al. (28) have reported that when pH is dropped from 7.1 to 5.5 in 2 $\underline{M}$ NaCl buffers, the heterotypic tetramer (H4, H3, H2A, H2B) converts to a mixture of the homotypic tetramer (H3, H4)$_2$ and H2A, H2B complexes. Similar pH effects may occur within

the nucleosome.   Parallel quaternary rearrangements of the inner histones within ν_1 may be the mechanism of the hydrodynamic and circular dichroic conformational transitions.

The present study illustrates that the techniques of laser Raman spectroscopy and circular dichroism complement each other when different solvents or additives are employed.   For example, due to the high UV absorbance of dimethyl sulfoxide, circular dichroism measurements were impossible, whereas useful "windows" were available for laser Raman spectroscopy.

ACKNOWLEDGEMENTS

*On leave from the National Institute of Radiological Sciences, Chiba-Shi, Japan.

REFERENCES

1.   Felsenfeld, G. (1978) Nature 271, 115–122
2.   Weintraub, H. and Groudine, M. (1975) Science 193, 848–856
3.   Garel, A. and Axel, R. (1976) Proc. Natl. Acad. Sci. USA 73, 3966–3970
4.   Olins, D. E., Bryan, P. N., Harrington, R. E., Hill, W. E., and Olins, A. L. (1977) Nucleic Acids Res. 4, 1911–1931
5.   Zama, M., Bryan, P. N., Harrington, R. E., Olins, A. L., and Olins, D. E. (1977) Cold Spring Harbor Symp. Quant. Biol. 42, in press
6.   Gordon, V. C., Knobler, C. M., Olins, D. E., and Schumaker, V. N. (1978) Proc. Natl. Acad. Sci. USA 75, 660–663
7.   Olins, A. L., Breillatt, J. P., Carlson, R. D., Senior, M. B., Wright, E. B., and Olins, D. E. (1977) in The Molecular Biology of the Mammalian Genetic Apparatus (P.O.P. T'so, ed.), pp. 211–237.   Elsevier/North-Holland, Amsterdam
8.   Olins, A. L., Carlson, R. D., Wright, E. B., and Olins, D. E. (1976) Nucleic Acids Res. 3, 3271–3291
9.   Thomas, Jr., G. J., Prescott, B., and Olins, D. E. (1977) Science 197, 385–388
10.   Thomas, Jr., G. J., (1976) Appl. Spectrosc. 30, 483–872.
11.   Zimmer, C. and Venner, H. (1966) Biopolymers 4, 1073–1079
12.   Zimmer, C., Luck, G., and Venner, H. (1968) Biopolymers 6, 563–574
13.   Lord, R. C. and Thomas, Jr., G. J. (1967) Spectrochim. Acta 23A, 2551–2591
14.   Chou, C. H. and Thomas, Jr., G. J. (1977) Biopolymers 16, 765–789
15.   Erfurth, S. E. and Peticolas, W. L. (1975) Biopolymers 14, 247–264
16.   Rimai, L., Maher, V. M., Gill, D., Salmeen, I, and McCormick, J. (1974)

Biochim. Biophys. Acta 361, 155–165

17. Mansy, S., Engstrom, S. K., and Peticolas, W. L. (1976) Biochem. Biophys. Res. Commun. 68, 1242–1247

18. Erfurth, S. E., Kiser, E. J., and Peticolas, W. L. (1972) Proc. Natl. Acad. Sci. USA 69, 938–941

19. Ivanov, V. I., Minchenkova, L. E., Schyolkina, A. K., and Poletayev, A. I. (1973) Biopolymers 12, 89–110

20. Gray, D. M., Taylor, T. N., and Lang, D. (1978) Biopolymers 17, 145–157

21. Herbeck, R., Yu, T.-J., and Peticolas, W. L. (1976) Biochemistry 15, 2656–2660

22. Nozaki, Y. and Tanford, C. (1965) J. Biol. Chem. 240, 3568–3573

23. Tanford, C., Buckley III, C. E., De, P. K., and Lively, E. P. (1962) J. Biol. Chem. 237, 1168–1171

24. Fox, J. W., Owens, D. P., and Wong, K.-P. (1978) Biochemistry 17, 1357–1364

25. Yu, N.-T. (1977) Crit. Rev. Biochem. 4, 229–278

26. Olins, D. É. (1978, in press) in The Structure and Function of Chromatin, International School of Biophysics, NATO Advanced Study Institute. Plenum Press, New York

27. Gordon, V. C., Knobler, C. M., Olins, D. E., and Schumaker, V. N. (1978) Biophys. J. 21, 66a

28. Weintraub, H., Palter, K., and Van Lente, F. (1975) Cell, 6, 85–110

29. Zama, M., Olins, D. E., Prescott, B., and Thomas, Jr., G. J. (1978) Biophys. J. 21, 66a